Computational Methods

The structure-data files (SDFs) and SMILES representations for compounds with antithrombotic properties, including quercetin (CID: 5280343), gallic acid (CID: 370), chlorogenic acid (CID: 1794427), catechol (CID: 289), caffeic acid (CID: 689043), coumaric acid (CID: 637542), and rosmarinic acid (CID: 5281792), were obtained from the PubChem database. The X-ray structure of the warfarin-VKOR-GFP fusion protein complex was retrieved from the Protein Data Bank (PDB ID: 6WV3) with the resolution 2.2 Å (Liu et al., 2021). Protein structure refinement was conducted using the Molecular Operating Environment (MOE) version 2019.0102, utilizing an enhanced refinement protocol designed to improve the stereochemical quality of the protein. Validated molecular docking (re-docking) was conducted using AutoDock, adopting a rigid-flexible docking approach with the Lamarckian genetic algorithm. Receptor and ligand preparation included assigning Gasteiger partial charges and identifying rotatable bonds, following established protocols (Shityakov and Forster, 2014; Shityakov et al., 2021). The binding site was centered on the co-crystallized ligand with Cartesian coordinates: x = -9.83 Å, y = 26.82 Å, z = 55.76 Å, and a grid box size of 60 x 60 x 60 Å. Structure-based (T_s) similarity scores were calculated using SMILES strings with the RDKit package. Descriptor-based (T_d) similarity scores utilized Lipinski's rule descriptors (molecular weight [MW], logP, hydrogen bond donors [HBD], hydrogen bond acceptors [HBA], and aromatic rings [AR]) alongside Gibbs free energy (ΔG_{bind}) values, as defined by:

$$T(A,B) = \frac{\sum(A_i \cdot B_i)}{\sum A_i^2 + \sum B_i^2 - \sum(A_i \cdot B_i)} \quad (eq.1)$$

where A_i and B_i represent descriptor values for molecules A and B. To address scale disparities (e.g., MW in hundreds, logP in small values, ΔG negative), descriptors were normalized to a [0, 1] range using:

$$X_{norm} = \frac{X - X_{min}}{X_{max} - X_{min}} \quad (eq.2)$$

Molecular visualizations were generated using PyMOL, and data plots were created with GraphPad Prism version 10.0 for enhanced clarity.

Results and Discussion

To identify the active compounds in Cannabis sativa seeds (CSS) contributing to the observed anticoagulant activity (Table 5), we performed re-docking analysis, achieving an RMSD of less than 2.0 Å between the co-crystallized ligand and its theoretical pose within the warfarin-VKOR-GFP complex (Figure 8A).

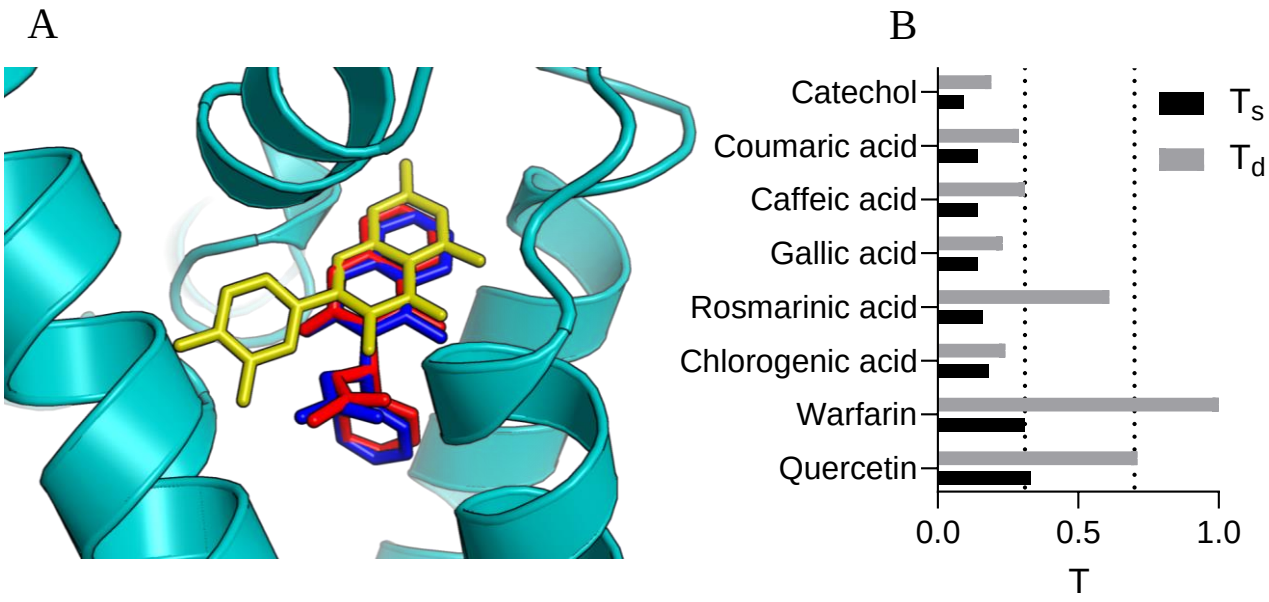

Figure 8: Validated molecular docking of the warfarin-VKOR complex, where the experimental and theoretical poses of warfarin are colored in blue and red, respectively. The protein structure depicted as cartoon model and quercetin molecule is colored in yellow (A). Structure-based (T_s) and descriptor-based (T_d) Tanimoto similarity functions for the Cannabis sativa compounds (B). The thresholds (0.3 and 0.7) are depicted as dotted lines.

As a result, rosmarinic acid (ΔG_{bind} = -10.91 kcal/mol), chlorogenic acid (ΔG_{bind} = -11.6 kcal/mol), and quercetin (ΔG_{bind} = -10.77 kcal/mol) exhibited higher binding affinities to VKOR than warfarin (ΔG_{bind} = -10.11 kcal/mol), suggesting their possible contribution to the prolonged APTT observed in *ex vivo* studies. However, no experimental evidence in the literature confirms direct interactions between polyphenolic compounds and VKOR that contribute to anticoagulant effects. For instance, liquiritigenin, a polyphenol from liquorice, modulates VKORC1 to inhibit ferroptosis in acute kidney injury, not directly affecting coagulation (Guo et al., 2024).

To enhance the specificity and selectivity of docking results, we employed a chemomolecular modeling approach integrating chemoinformatics and molecular docking. The 4-hydroxycoumarin moiety was used as a reference for structural similarity calculations because this molecular component is a key part of the warfarin molecule responsible for its bioactivity (Liu et al., 2021). Structure-based (T_s) analysis using the 4-hydroxycoumarin substructure revealed the same structural similarity of warfarin and quercetin to this molecular fragment (Figure 8B). Conversely, descriptor-based (T_d) analysis, incorporating molecular properties and binding affinities (Table 7), confirmed that quercetin also exhibited the highest similarity (T_d = 0.71) to warfarin, slightly exceeding the established similarity ($T \geq 0.7$) threshold (Mellor et al., 2019; Kleandrova et al., 2021). Overall, these findings suggest that quercetin may exhibit predicted structural and

functional similarities with warfarin, underscoring the need for further experimental validation to confirm its potential anticoagulant role.

Table 7: Molecular properties and binding affinities (ΔG_{bind} in kcal/mol) of analyzed ligands determined from C. sativa.

Name	**MW**	**LogP**	**HBD**	**HBA**	**AR**	**ΔG_{bind}**
Quercetin	302.24	1.99	5	7	3	-10.77
Gallic acid	170.12	0.5	4	4	1	-6.42
Chlorogenic acid	354.31	-0.64	6	8	1	-11.6
Catechol	110.11	1.09	2	2	1	-5.39
Caffeic acid	180.16	1.19	3	3	1	-7.07
Coumaric acid	164.16	1.49	2	2	1	-6.04
Rosmarinic acid	360.32	1.76	5	7	2	-10.91
Warfarin	308.33	3.61	1	4	3	-10.11

Data Availability Statement

The data and code supporting the reproducible results of this computational modeling and simulation study are openly available in the GitHub repository at: https://github.com/virtualscreenlab/VKOR/.

References

Liu, S., et al. (2021). "Structural basis of antagonizing the vitamin K catalytic cycle for anticoagulation." Science **371**(6524).

Shityakov, S. and C. Forster (2014). "In silico predictive model to determine vector-mediated transport properties for the blood-brain barrier choline transporter." Adv Appl Bioinform Chem **7**: 23-36.

Shityakov, S., et al. (2021). "Scaffold Searching of FDA and EMA-Approved Drugs Identifies Lead Candidates for Drug Repurposing in Alzheimer's Disease." Front Chem **9**.

Guo, R.-Z., Li, J., Pan, S.-K., Hu, M.-Y., Lv, L.-X., Feng, Q., Qiao, Y.-J., Duan, J.-Y., Liu, D.-W., & Liu, Z.-S. (2024). Liquiritigenin, an active ingredient of liquorice, alleviates acute kidney injury by VKORC1-mediated ferroptosis inhibition. *The American Journal of Chinese Medicine*, *52*(5), 1507–1526.

Mellor, C. L., et al. (2019). "Molecular fingerprint-derived similarity measures for toxicological read-across: Recommendations for optimal use." Regul Toxicol Pharmacol **101**: 121-134

Kleandrova, V. V., et al. (2021). "QSAR Modeling for Multi-Target Drug Discovery: Designing Simultaneous Inhibitors of Proteins in Diverse Pathogenic Parasites." Front Chem **9**: 634663.